ELSEVIER

International Journal of Mass Spectrometry 219 (2002) 171–187

International Journal of Mass Spectrometry

www.elsevier.com/locate/ijms

Charge state dependent fragmentation of gaseous protein ions in a quadrupole ion trap: bovine ferri-, ferro-, and apo-cytochrome *c*

Brian J. Engel, Peng Pan, Gavin E. Reid, J. Mitchell Wells, Scott A. McLuckey*

1393 Brown Laboratory, Department of Chemistry, Purdue University, West Lafayette, IN 47907-1393, USA

Received 14 August 2001; accepted 21 December 2001

Abstract

The dissociation behavior of bovine ferri-, ferro-, and apo-cytochrome *c* ions formed by electrospray ionization has been studied as a function of precursor ion charge state under quadrupole ion trap collisional activation conditions. Tandem mass spectrometry data collected under solution conditions in which the oxidation state of the heme-iron is known show that cytochrome *c* ions dissociate by oxidation state dependent channels. Dissociation of precursor ions in the oxidized form [Fe(III)heme] yields predominantly b- and y-type ion backbone cleavages with preferential cleavages observed C-terminal to basic residues including lysine, arginine and histidine, C-terminal to aspartic and glutamic acids as well as N-terminal to proline. At the highest charge states studied, an abundant Leu–Met cleavage is apparent. The relative contribution of each type of fragmentation was found to be a function of precursor ion charge state. Dissociation of cytochrome *c* ions in the reduced form [Fe(II)heme] show, in addition to backbone cleavages, loss of protonated heme, which dominates the product ion spectrum for the $[M + 7H]^{7+}$ and $[M + 8H]^{8+}$ precursor ion charge states. Apo-cytochrome *c* ions dissociate via similar fragmentation channels to those observed in the product ion spectra for the oxidized form of cytochrome *c*. The results presented in this study are expected to reflect predominantly first generation cleavage products from cytochrome *c* precursor ions in the temperature range of 500–650 K. (Int J Mass Spectrom 219 (2002) 171–187)

Keywords: Electrospray; Quadrupole ion trap; Cytochrome *c* ions; Ion/ion reactions; Collisional activation

1. Introduction

With the advent of desorption [1,2] and spray ionization techniques [3], mass spectrometry has been extended to the study of large, gaseous biomolecule-ions, including those derived from proteins and oligonucleotides. Cytochrome *c*, a peripheral membrane metalloprotein on the outer surface of the inner mitochondrial membrane of aerobically respiring organisms, is perhaps, the most extensively studied protein using mass spectrometry. A wide array of mass spectrometric and related techniques have been applied to probe structural aspects and reactivities of gaseous ions derived from cytochrome *c*. Examples include the study of ion/molecule proton transfer reactions [4–9], attachment of hydroiodic acid [10], hydrogen/deuterium exchange studies [11–14], as well as studies examining ion mobility [14–19], collision cross-section [20,21], and the electron capture dissociation of cytochrome *c* ions in the gas-phase [22–24]. The collision-induced dissociation (CID) behavior of gaseous cytochrome *c* ions has also been reported

* Corresponding author. E-mail: mcluckey@purdue.edu

1387-3806/02/$ – see front matter
PII S1387-3806(02)00562-6

for a limited range of precursor ion charge states using triple quadrupole tandem mass spectrometry [25–27], and both CID [28] and infrared multiphoton dissociation [29] has been effected in Fourier transform-ion cyclotron resonance (FT-ICR) tandem mass spectrometers.

The unimolecular dissociation behavior of gaseous protein ions is of practical interest from the standpoint of protein identification and characterization. Dissociation patterns of whole protein ions can yield primary sequence information of use in the identification and characterization of unknown proteins using the "top-down" approach [30]. This strategy involves the dissociation of whole protein ions, thereby minimizing labor intensive sample preparation techniques associated with the "bottom-up" approach, whereby peptide ions derived from solution phase proteolytic digestion of the protein of interest are dissociated for subsequent identification [31].

It is widely known that precursor ion charge state can play a major role in the dissociation of gaseous peptide ions [32] and that precursor ion charge state effects are also commonly observed with gaseous protein and oligonucleotide ions. We have recently reported, for example, the charge state dependent fragmentation behavior of gaseous insulin [33], hemoglobin β-chain [34], ubiquitin [35], and apomyoglobin [36] ions in a quadrupole ion trap over wide range of precursor ion charge states. These studies were facilitated by the use of ion/ion proton transfer reactions [37] for both precursor and product ion charge state manipulation [38]. Significant differences were observed for high, intermediate, and low charge state precursor ions. However, given the diversity of structural motifs and post-translational modifications associated with proteins, factors other than precursor ion charge and protein primary structure are expected to play roles in determining the favored dissociation channels associated with gaseous protein ions. Such factors include possible effects arising from secondary and tertiary structures, the identities and locations of post-translational modifications, and the conditions under which precursor ions are activated. Given the relatively small data set available for the charge state dependent fragmentation behavior of gaseous whole protein ions, it remains unclear how important secondary and tertiary structural effects are, for example. As a consequence, it is unclear what structural information might be derived from the product ion spectrum of a particular charge state of a gaseous protein ion. From a practical perspective, limited structural information may be sufficient to identify a protein; however, in applications requiring protein characterization, as in the identification and localization of post-translational modifications, more extensive information may be required. Given that the primary sequence information available from gaseous protein ions via dissociation is sensitive to variables such as precursor ion charge state, ion activation conditions, etc., it is important to understand the unimolecular chemistry of these ions over a wide range of conditions.

In this work, the charge state dependent gas-phase dissociation behavior of bovine ferri-, ferro-, and apo-cytochrome *c* ions, formed via conventional or nano-electrospray ionization from a variety of solution compositions, has been examined under ion trap collisional activation conditions. In a recent communication, we reported on the oxidation state dependence of the fragmentation of a limited set of gaseous cytochrome *c* charge states [39]. That work focused on the loss of the heme group as a signature of iron oxidation state. In this paper, we focus on the charge state (z) dependence of the peptide backbone cleavages from ions containing the heme group as well as those from which the heme group has been removed.

2. Experimental

Bovine heart cytochrome *c* was obtained from Sigma Chemical Co., St. Louis, MO, and was used without further purification. Perfluoro-1,3-dimethylcyclohexane (PDCH), and sodium L -ascorbate were purchased from Aldrich, Milwaukee, WI. Working solutions were prepared daily by dilution of 10 mg/mL stock solutions of cytochrome *c* (prepared in 18 MΩ water) to a final concentration of 5–10 μM.

Solutions of ferri-, ferro-, and apo-cytochrome *c* were introduced into a quadrupole ion trap mass spectrometer via an electrospray interface, which has been described previously [40]. Solutions containing the protein in its oxidized form [Fe(III)heme] were electrosprayed from a solution composition of 85% methanol, 14% water, and 1% acetic acid. Reduced protein solutions [Fe(II)heme] containing 1 mM sodium L -ascorbate were prepared in 1% acetic acid and were nano-electrosprayed through drawn borosilicate glass capillaries using a stainless steel wire inserted through the back of the capillary to apply the electrospray potential. Apo-cytochrome *c* was prepared from holo-cytochrome *c* via the modified silver sulfate method of Paul [41] and purified using reversed-phase HPLC. Solutions for nano-electrospray of the apo-protein were prepared in 50% methanol and 49% water containing 1% acetic acid prior to introduction to the mass spectrometer.

Protein ions were injected into the trap for a period ranging from 0.1 to 0.6 s at an applied potential of 3.5–4.0 kV when using conventional electrospray, and 1.0–1.4 kV when using nano-electrospray. Precursor ions of charge states lower than those obtained directly from electrospray ionization were formed through ion/ion proton transfer reactions. Charge state reduction was effected by reacting the initial protein ion population with singly charged PDCH anions that were injected through a 3-mm hole in the ring electrode following formation via an atmospheric sampling glow discharge ionization source as described previously [42]. Isolation of the precursor ion of interest was effected using a series of resonance ejection ramps, each consisting of a sweep of the drive rf amplitude while simultaneously applying a single frequency sine wave of $\sim$15 V_{p-p} across the end-caps at a frequency chosen to eject ions of mass to charge higher or lower than that of the ion of interest [43]. Cooling steps of 20–30 ms were added following ion injection and all isolation ramps to effectively cool trapped ions to the center of the trap in the event that ions were internally excited during the ion accumulation or ion isolation processes. Precursor ions were subjected to CID via single-frequency resonance excitation in the presence of 1 mTorr of He bath gas by applying a sine wave of amplitude 250–600 mV_{p-p} to the end-caps with a frequency in resonance with the axial secular frequency of the ion of interest [44]. The amplitude of the excitation frequency was chosen such that the product ion spectrum gave the best signal-to-noise ratio while leaving a sufficient precursor ion population to aide in the analysis of post-ion/ion spectra. The resulting product ion population was then subjected to ion/ion proton transfer reactions via reactions with negative PDCH ions for a period of 50–100 ms to convert the product ion charge states to predominantly +1. Prior to mass analysis, negative PDCH ions were ejected from the trap by applying a ramp of the drive rf amplitude to eject ions of *m*/*z* less than 640 to avoid deleterious effects on positive ion detection [45]. Mass analysis of the product ion spectrum was then effected via single-frequency resonance ejection by applying a 17 kHz sine wave of amplitude 1.5 V_{p-p} across the end-caps, where ions were ejected sequentially from the trap in order of lowest to highest *m*/*z* [46]. Mass scale calibration for post-ion/ion data was performed by using post-ion/ion data acquired under conditions in which no precursor ion activation was performed. Spectra presented here are the result of an average of 1000 individual mass analysis scans.

3. Results and discussion

To place the results described herein into context with data reported from other studies of gaseous cytochrome *c* ions, it is instructive to consider the conditions under which the precursor ions were activated. Ion trap collisional activation is a slow heating process [47] whereby the precursor ion population undergoing resonance excitation in the presence of the helium bath gas reaches a steady-state internal energy condition greater than that of the ions stored in the absence of resonance excitation. In the absence of fragmentation, the new steady-state internal energy distribution has a Boltzmann distribution and can be described with a temperature [48]. Provided the

microscopic rates of fragmentation are smaller relative to the rates for ion activation and deactivation via collisions and infrared photon absorption/emission, the internal energy distribution of a resonantly excited ion population undergoing fragmentation can also be approximately described with a temperature. Therefore, the ion trap collisional activation data represent fragmentation from a quasi-thermal precursor ion population at a temperature greater than that of the bath gas. All of the cytochrome *c* ions in this study were subjected to resonance excitation for a period of 300 ms with the overall dissociation rates falling in the range of 1–10 s^{-1}, with the majority of ions falling in the 1–5 s^{-1} dissociation rate range. Assuming Arrhenius activation parameters of $E_a = 1.2$ eV and $A = 10^{12}\ s^{-1}$, which are values well within the range measured for gaseous bovine ubiquitin ions [49], the dissociation rates associated with the results described here are consistent with precursor ions in the effective temperature range of 500–650 K. While this is simply an estimate based on measurements of another covalently bound protein, it puts into perspective the conditions to which the ions have likely been exposed.

A second important point regarding the nature of the cytochrome *c* product ion spectra collected in this work is that the first generation product ions are not subjected to resonance excitation and are, therefore, actively cooled via collisions with the room temperature helium bath gas. Based on modeling studies of the removal of excess ion internal energy under these conditions [50], the cooling rates associated with the cytochrome *c* product ions are expected to be on the order of $10^2\ s^{-1}$ (i.e., greater than the precursor ion dissociation rates). Previous studies with protonated leucine enkephalin indicate that with room temperature helium, the likelihood for the observation of second generation product ions is very low, with the exception of those formed from first generation product ions that are significantly less kinetically stable than the precursor ion [51]. Therefore, the conditions used to generate product ion spectra here lead to the preferential observation of first generation product ions. As a result, a large majority of the product ions can be regarded as arising from competitive fragmentation channels from the dissociation of the selected precursor ion. Ion trap resonance excitation of the precursor ion preferentially yields first generation products that facilitate comparison of the relative importance of the various possible competitive dissociation channels.

While the body of observations from the studies of gas-phase, whole protein ion dissociations is still relatively small, commonalities with known gaseous peptide ion dissociations are observed, including a variety of observed preferential cleavages for which dissociation mechanisms may be readily rationalized. In the event that these and subsequent observations lead to the discovery of dissociation patterns which are general for a wide assortment of protein ions, database sequence searching algorithms might be devised to identify and, possibly, characterize unknown proteins based on protein ion dissociation behavior.

3.1. The role of Fe oxidation state in the dissociation of bovine holo-cytochrome c ions

In a recent communication we noted that, depending upon precursor ion charge state, the gas-phase dissociation channels of holo-cytochrome *c* ions can exhibit striking differences as a result of the oxidation state of the heme-iron [39]. In this study, we observed the electrochemical reduction of ferri-cytochrome *c* ions occurring in the nano-electrospray assembly. The reduction of ferri-cytochrome *c* in positive ion nano-electrospray was noteworthy in that positive ion electrospray is generally an oxidizing environment [52]. However, evidence was presented which suggests that oxidation of iron in the stainless steel wire used to make electrical contact with the solution in the nano-spray emitter liberates Fe(II) into solution which, in turn, can undergo homogeneous redox chemistry with ferri-cytochrome *c* to yield ferro-cytochrome *c*. Under these conditions, the appearance of ferro-cytochrome *c* from a solution originally containing ferri-cytochrome *c* generally required nano-spraying for several minutes, and was dependent upon the proximity of the wire end to the capillary tip. Reduced cytochrome *c* ions could be observed essentially immediately, however, if the ferro-cytochrome *c*

was already present in solution along with a reducing agent, such as sodium L -ascorbate.

Differences in product ion spectra derived from ferri- and ferro-cytochrome *c* precursor ions are most apparent for the +7 and +8 charge states. For the $[M + 7H + Fe(II)heme]^{7+}$ and the $[M + 8H + Fe(II)heme]^{8+}$ ferro-cytochrome *c* precursor ions, the overwhelmingly dominant dissociation channel observed is due to loss of the heme group. In contrast, the dissociation channels observed upon activation of $[M + 6H + Fe(III)heme]^{7+}$ and $[M + 7H + Fe(III)heme]^{8+}$ ferri-cytochrome *c* precursor ions are the formation of product ions resulting predominantly from amide bond cleavages. These observations are illustrated by a comparison of the post-ion/ion product ion spectra of the +8 precursor ion charge states of reduced and oxidized forms of the protein following reduction of the charge states of the product ions and residual parent ions largely to +1 via ion/ion proton transfer reactions, as provided in Fig. 1. The reduced precursor ion ($[M+8H+Fe(II)heme]^{8+}$) fragments are formed mainly through the heme loss channel, although amide bond cleavages resulting in complementary N-terminal b-type, and C-terminal y-type product ions are also represented, albeit at relatively low abundance. The "pre-ion/ion," or conventional product ion spectrum (data not shown) indicated that the heme group was lost as a charged species. Mass measurement of the charged heme product ion indicated virtually 100% formation of $[Fe(II)heme + H]^+$, as opposed to $[Fe(III)heme]^+$. Essentially identical observations can be made from a comparison of the $[M+7H+Fe(II)heme]^{7+}$ precursor ions [39]. However, the heme loss channel for both $[M + 9H + Fe(II)heme]^{9+}$, the highest charge state for which MS/MS data for ferro-cytochrome *c* ions could be obtained, and $[M+6H+Fe(II)heme]^{6+}$ ions was significantly less prominent than for the $[M + 8H + Fe(II)heme]^{8+}$ and $[M + 7H + Fe(II)heme]^{7+}$ ions. Furthermore, at precursor ion charges of +5 and below, the dominant dissociation channels observed for ferro-cytochrome *c* ions are amide bond cleavages very similar to those observed in the product ion spectra of the oxidized protein.

With the resolving power of the ion trap used in these studies, it is not possible to determine the purity of the selected precursor ions. That is, the product ion spectra can reflect contributions from at least

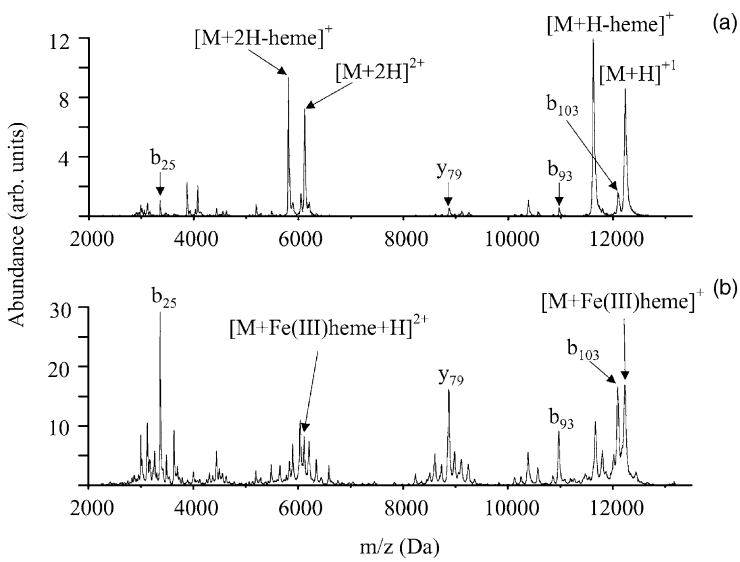

Fig. 1. (a) Post-ion/ion MS/MS of the $[M + 8H + Fe(II)heme]^{8+}$ precursor ion of ferro-cytochrome *c* formed via electrochemical reduction in the nano-electrospray assembly. (b) Post-ion/ion MS/MS of the $[M + 7H + Fe(III)heme]^{8+}$ precursor ion of ferri-cytochrome *c*.

some of each precursor ion oxidation state within a given precursor ion charge state. Such a scenario might account for the small degree of protonated heme loss observed from nominal ferri-cytochrome *c* precursor ion populations. That is, some degree of contamination of the ferri-cytochrome *c* precursor ion population by ferro-cytochrome *c* ions of the same charge state cannot be precluded. Furthermore, amide bond cleavage products observed in the product ion spectrum of Fig. 1a, which is that of the nominal $[M + 8H + Fe(II)heme]^{8+}$ precursor ion, might arise, at least in part, from contamination by the $[M + 7H + Fe(III)heme]^{8+}$ precursor. Both the identities and relative abundances of the amide bond cleavage products of the reduced ion match closely to those observed in Fig. 1b, the product ion spectrum of the $[M + 7H + Fe(III)heme]^{8+}$ precursor ion where amide bond cleavage is preferred. It is also expected that backbone cleavages and heme loss from a given oxidation state are competing processes. This leaves open to speculation the underlying reason(s) why the +7 and +8 charge states of the reduced protein, in particular, fragment via loss of heme. Perhaps the presence of a net positive charge on the heme group of ferri-cytochrome *c* confers stability to the heme in the oxidized ion, relative to that of the reduced ion. This might arise simply as a result of solvation of the charge by the protein scaffolding. Alternatively, perhaps the additional charge on the heme iron in ferri-cytochrome *c* minimizes the extent to which intramolecular proton transfer occurs to locations near the heme group that might catalyze cleavage of the thioether linkages covalently binding the prosthetic group to the protein backbone. While no firm conclusions can be drawn from the data presented here, the overall charge state fragmentation behavior of the ferro-cytochrome *c* precursor ions are consistent with a proton mobility picture that, at least qualitatively, is consistent with the charge state fragmentation behavior of other protein ions studied systematically to date. That is, proton mobility tends to be inhibited at both high and low charge states, although for different reasons, and is maximized at intermediate charge states. At low charge states, protons tend to reside on the most basic residues and can be stabilized by multiple solvating interactions within the protein, thereby minimizing proton mobility in activated ions. At high charge states, the tendency to minimize Coulomb repulsion arising from the large number of excess protons tends to inhibit proton mobility. At intermediate charge states, neither Coulomb forces nor strong proton binding dominate such that intramolecular proton transfer is minimally inhibited. The fact that ferro-cytochrome *c* ions show a marked preference for protonated heme loss at charge states +8 and +7 but a lesser tendency for heme loss at +9 and +6 and lower may be related to the issue of proton mobility within the protein.

A final consideration in the discussion of oxidation state dependent fragmentation behavior of holo-cytochrome *c* ions deals with the possible role of *gas-phase* redox chemistry associated with the ion/ion reactions. Ion/ion reactions have been used to form precursor ion charge states lower than those yielded directly by electrospray. Multiply charged protein cations have been observed to react with anions derived from glow discharge of PDCH only via proton transfer [53]. The occurrence of electron transfer from singly charged anionic species to multiple charged cations has been observed previously for highly conjugated cationic (non-protein) species only [42]. However, in the case of metalloproteins, the possibility of electron transfer to the metal center must be considered. Comparison of the product ion spectrum derived from a +8 precursor ion population formed directly from the ESI source from a solution containing ferri-cytochrome *c* with that of a +8 precursor ion population formed from higher charge states of ferri-cytochrome *c* via ion/ion reactions with PDCH anions shows that the dissociation of these two species are identical (i.e., both appear as the spectrum of Fig. 1b). This result indicates that no observable reduction of high charge state ferri-cytochrome *c* ions occurs as a result of ion/ion reactions when forming the +8 precursor ion. This suggests that the PDCH anions react preferentially via proton transfer, as opposed to electron transfer. Similar experiments could not be conducted for charge states of +6 and lower since they are not formed directly via electrospray.

Electron transfer to the metal center of the heme group may compete with proton transfer when the number of available protons for abstraction is small. Therefore, the possibility exists for some degree of reduction of ferri-cytochrome *c* ions as a result of ion/ion reactions for the +6 and lower charge states. However, as all cytochrome *c* ions below the +6 charge state, regardless of initial oxidation state, tend to fragment at amide bonds, the fragmentation behavior of the low charge state precursor ions cannot be used to draw conclusions regarding this possibility.

3.2. Charge state dependent amide bond cleavages of bovine holo-cytochrome c ions

As noted above, for the precursor ion charge states for which data could be obtained for both ferri- and ferro-cytochrome *c* ions, the identities and relative abundances of product ions arising from amide bond cleavages are very similar. Therefore, a description of the data for either holo-cytochrome *c* system summarizes the backbone cleavage phenomenology noted for both oxidation states. The observed fragmentation behavior of the cytochrome *c* system adds to the growing body of observations regarding the charge state dependent fragmentation behavior of proteins. Many of the same trends noted for other proteins, such as apomyoglobin [35] and ubiquitin [36], are observed in the charge state dependent backbone fragmentation reactions of cytochrome *c*. For all of these protein systems, the dissociation behaviors of whole protein ions are consistent with what is currently known about the fragmentations of small peptides under low energy collisional activation conditions. For example, fragmentation appears to be dominated primarily via cleavages to yield b- and y-type ions. The sequence specific cleavages often observed in protonated peptides are also often observed with proteins as well. Furthermore, the identities and abundances of product ions can be strongly influenced by precursor ion charge state. The emerging trends for charge state dependent protein ion dissociation can be rationalized qualitatively within the framework of the so-called "mobile proton model" [32]. Many of the most frequently observed, or facile protein backbone cleavages presented within this work may be rationalized by the mechanistic arguments that are made for sequence specific cleavages of small peptides using this model. The phenomenology noted specifically for peptide bond cleavages in holo-cytochrome *c* ions is summarized below ranging from low precursor ion charge states to the highest accessible in these experiments. Bovine heart cytochrome *c* contains a total of 23 basic residues, including 18 lysines, three histidines, and two arginines with its N terminus being acetylated (see Scheme 1). With the current instrumental apparatus and spray solution compositions, the highest charge state observed is that of the $[M + 16H + Fe(III)heme]^{17+}$ ion, but the $[M + 14H + Fe(III)heme]^{15+}$ ion is the highest charge state for which sufficient parent ion signal was available to conduct the tandem MS ion/ion experiment. The lowest precursor ion charge state for which acceptable product ion signal-to-noise ratios could be obtained was the +3 charge state.

3.3. Low charge state holo-cytochrome c precursor ions charge states (<+5)

The fragmentation behavior of the lowest cytochrome *c* ion charge states under ion trap collisional activation conditions shows commonalities with those observed for previously studied protein ions [34–36]. Principal among these is the tendency to show losses of small molecules, such as water and/or ammonia, sometimes in conjunction with amide bond cleavages. A practical problem arises from the competition between ion activation and ion ejection common to all ion trap collisional activation experiments. The ion acceleration process necessary for collisional activation can also give rise to ejection of the precursor ions from the ion trap. In the case of ions of high mass-to-charge ratio, such as protein ions of low charge state, only relatively shallow trapping wells can be effected with the rf trapping amplitudes available from the ion trap electronics. Therefore, CID can only be induced, if at all, by use of relatively low resonance excitation amplitudes. An often effective strategy is to employ relatively long activation times so that fragmentation

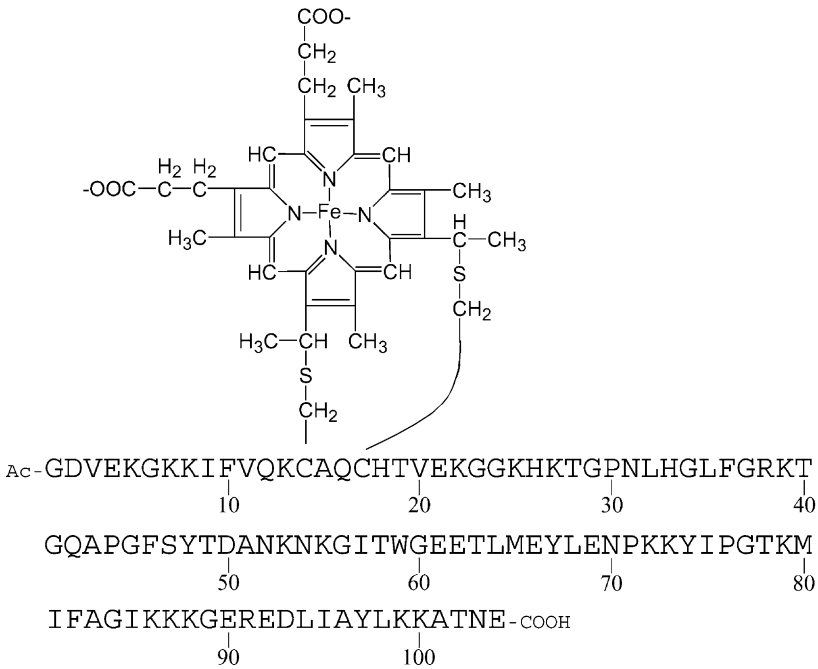

Scheme 1.

reactions of relatively low rates can be observed. Such slow processes are commonly associated with uninformative small molecule losses; however, ion activation conditions alone cannot account for the tendency to observe prominent small molecule losses from low charge state protein ions, as the activation conditions used for the higher charge states also lead to extensive small molecule losses in low charge state ions. Fig. 2 shows the post-ion/ion product ion spectrum derived from the $[M + 3H + Fe(II)heme]^{3+}$ ion

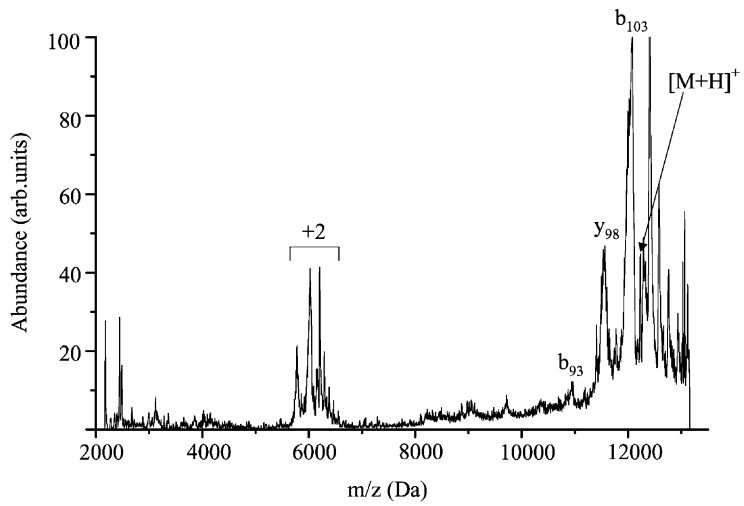

Fig. 2. Post-ion/ion MS/MS of the $[M + 3H + Fe(II)heme]^{3+}$ precursor ion of ferro-cytochrome *c*.

of ferro-cytochrome *c*. A number of products presumably arising from amide bond cleavages are observed but the signals are broad, reflecting contributions from sequential fragmentations. By far, the most abundant product ion signals are observed at *m*/*z* ratios slightly below that of the precursor ion and are consistent with the loss of several small molecules, presumably water and/or ammonia, in some cases in conjunction with amide bond cleavages. (Peaks appearing at higher *m*/*z* than the $[M + H]^+$ ion are due to the difficulties encountered in performing precursor ion isolation at high *m*/*z* values. As a result of the combination of relatively low trapping well-depths and low frequency dispersion of ions at high *m*/*z*, it is difficult to isolate high *m*/*z* parent ions with high efficiency in an *m*/*z* window normally used for low *m*/*z* parent ions. Therefore, the ion isolation window was expanded on the high *m*/*z* side to avoid ambiguities in interpreting post-ion/ion reaction product ion signals, which appear only on the low *m*/*z* side of the residual parent ion signal.) The observed small molecule losses have been rationalized on the basis of intramolecular charge solvation at sites of relatively high basicity. Intramolecular solvation of charge at relatively few basic sites tends to maximize the possibility for small molecule losses of the sort reported, for example, for ammonia loss from singly-protonated bradykinin. Williams and coworkers have shown that this process occurs when the two arginine residues of bradykinin solvate the charge [54]. This type of behavior tends to minimize the structural information available from the lowest charge state protein ions, at least under conventional ion trap collisional activation conditions. The observation of small molecule losses in conjunction with amide bond cleavages can arise from the ion activation conditions used for high *m*/*z* ions. Due to the low frequency dispersion of ions at high *m*/*z* for a given set of ion storage conditions, the *m*/*z* band-width of ions activated with single frequency resonance excitation is greater at high *m*/*z* than at low *m*/*z*. Therefore, first generation product ions formed by small molecule loss can also undergo ion acceleration if they fall within the finite *m*/*z* band-width of ions determined by the frequency and amplitude of the resonance excitation voltage. Unfortunately, it is not possible with the present apparatus to adjust ion storage conditions such that each parent ion charge state can be activated at the same frequency. The lowest charge state parent ions were activated under conditions of relatively low ion frequency dispersion.

3.4. Intermediate holo-cytochrome c precursor ion charge states (+5 to +9)

Amide bond cleavages compete with small molecule losses much more effectively for intermediate-to-high precursor ion charge states than for low precursor ion charge states. For the former, both products arising from an amide bond cleavage typically carry at least one charge. Therefore, each appears in the product ion spectrum, provided that they fall within the mass-to-charge range available for product ion storage. In the post-ion/ion MS/MS spectrum of the $[M + 5H + Fe(III)heme]^{6+}$ precursor ion, the dominant fragmentation channel yields the b_{50}/y_{54} complementary pair denoted in the upper left panel of Fig. 3. The relative frequency of occurrence of this C-terminal Asp cleavage with respect to all other observed amide bond cleavages is more clearly displayed in the upper right panel of this figure, depicting the summed b and y ion histogram derived from the tandem MS data in the panel to its left. In this and subsequent histograms, the frequency of each dissociation channel represents the sum of the abundances of the singly charged b- and y-type complementary ion pairs, normalized to the sum of the ion signals from the observed singly charged product ions.

In the case of the intermediate charge state +6 precursor ion, the occurrence of the dominant Asp cleavage is consistent with observations made with other protein ions of intermediate charge [34–36] as well as peptide ions in which proton mobility is low. In this circumstance, the initiation of amide bond cleavage is effected via bond activation by the carboxylic acid of the Asp side chain [55–58]. This charge remote amide bond fragmentation tends to be favored when proton mobility is relatively low. For peptide ions, it is often observed when the number

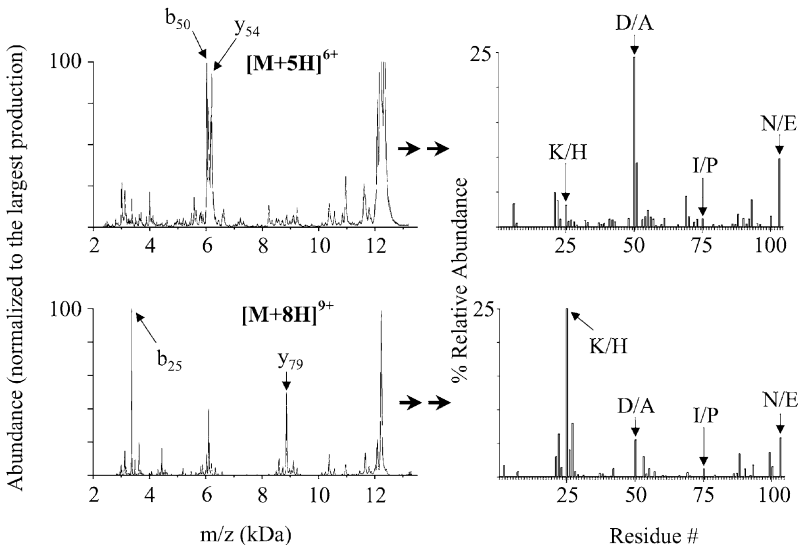

Fig. 3. On the left-hand side is shown the post-ion/ion MS/MS of the $[M+5H+Fe(III)heme]^{6+}$ and $[M+8H+Fe(III)heme]^{9+}$ precursor ions of ferri-cytochrome *c* where the complementary ion pair of the most dominant amide bond dissociation is labeled. On the right-hand side is shown the summed b and y ion plots corresponding to the MS/MS data at left, where four of the major dissociation channels observed throughout the charge states studied are labeled. The *y*-axis represents the sum of the ion abundances corresponding to the dissociation of a given amide bond normalized to the sum of the observed product ion abundances.

of arginine residues is equal to or greater than the number of ionizing protons. In such a case, it is argued that the protons are sequestered on the highly basic arginine side chain(s) (PA = 235.7 kcal/mol for guanidine) [59] thereby minimizing contributions from non-specific amide cleavages that are catalyzed by proton transfer to backbone carbonyl groups. Not surprisingly, peptide bond cleavages initiated by the carboxylic acid side chain of Glu are also prominent in the product ion spectrum of the +6 charge state, where six of the nine total Glu residues cleave on the C-terminal side. Charge directed fragmentation of the +6 ion at basic sites where protons are expected to be located are also observed, with 2/2 Arg, 14/18 Lys, and 2/3 His residues yielding backbone cleavages C-terminal to the implicated residues. While these basic site cleavages account for 20% of the total observed fragmentation, some 41% is represented by C-terminal Asp and Glu channels (see Table 1). The MS/MS spectrum of the +6 precursor ion, as

Table 1
Relative contributions of acidic, basic and proline residues in the dissociation of ferri- and apo-cytochrome *c* ions in a QIT

z	Acidic residues holo(apo)	Basic residues holo(apo)	Proline holo(apo)	Non-specific cleavages holo(apo)
6	41 (46)	20 (33)	4 (6)	35 (15)
7	30 (25)	45 (51)	6 (7)	19 (18)
8	24 (18)	54 (45)	5 (17)	17 (21)
9	14 (13)	73 (56)	2 (11)	11 (20)
10	14 (11)	41 (35)	37 (31)	7 (23)
11	8 (12)	37 (33)	41 (35)	15 (20)
12	18 (15)	37 (27)	24 (23)	21 (36)
13	21 (17)	30 (27)	21 (15)	29 (42)
14	23 (20)	28 (22)	23 (16)	27 (41)
15	20 (20)	33 (17)	11 (12)	37 (51)

with most other charge states examined, shows an abundance of non-specific cleavages as well, although most segments of the protein in which non-specific cleavages occur are either centered around basic residues or residues such as Asp, Glu, or Pro. Note that signals labeled N/E, which arise from a cleavage between Asn and Glu at the C terminus, might also arise from side chain cleavages, and/or multiple losses of small molecules. The proximity of these signals to the *m*/*z* value of the parent ion makes this assignment more ambiguous than the other amide bond cleavage assignments.

While many of the cleavages present in the +6 post-ion/ion spectrum are also present in that of the +9 charge state of ferri-cytochrome *c*, a significant difference in the most prevalent dissociation channel is observed, as shown in the lower left panel of Fig. 3, where the b_{25}/y_{79} complementary pair dominates. The tendency for Lys–His cleavage has been noted in the dissociation of apomyoglobin ions [36] and occurs at intermediate charge states, with respect to the total number of available basic sites, for both the cytochrome *c* and myoglobin systems. Mechanisms of peptide bond cleavage induced by a proton that is solvated by a consecutive Lys–His pair have been proposed [36], where the relatively high basicity of this site leads to the initiation of localized charge directed cleavages. The transition between dominant dissociation channels of the +6 and +9 charge states of ferri-cytochrome *c* occurs gradually, which is most easily observed in the dissociation map of ferri-cytochrome *c* in Fig. 4. In this figure, the percent relative abundance represents the summed b and y ion abundances observed upon CID of a particular precursor ion, where this scale is normalized to the total abundance of observed fragments. As shown here, the contribution of the b_{50}/y_{54} C-terminal Asp channel falls to an approximately constant level by the +9 charge state, where the Lys–His channel maximizes. In the tandem mass spectrum of the +9 ion, approximately 73% of the amide bond fragmentation is accounted by cleavages C-terminal to basic residues, greater than 50% of which is accounted by the b_{25}/y_{79} channel. For the +9 precursor ion, only 14% of the observed fragmentation is initiated by acidic Asp and Glu residues.

3.5. High holo-cytochrome c precursor ion charge states (+10 to +15)

Since the range of available charge states formed directly via electrospray of sufficient abundance for MS/MS and ion/ion chemistry in this work is limited to a maximum charge of +15, those precursor ions of charge in the range of approximately +10 up to +15 are designated herein as high charge states. A sharp transition occurs between the +9 and +10 charge states where the b_{75}/y_{29} N-terminal proline fragmentation channel dominates the latter product ion spectrum and remains the single most prominent dissociation channel through the +14 charge state (see Fig. 4) while the frequency of the Lys–His channel falls to an approximately constant level by the +12 charge state. The relative frequency of occurrence of the b_{75}/y_{29} channel in the +10 charge state (37% of the total fragmentation) is roughly 30 times that of its appearance in the MS/MS of the +9 ion, making this the most dramatic change in dissociation channels observed between consecutive charge states under CID conditions.

Given the high dimensionality associated with whole protein ion dissociation and the level at which protein ion dissociation behavior is currently understood, it is difficult to draw definitive conclusions regarding the underlying cause for such a major change in the dominant dissociation channel. However, it is interesting to note that ion mobility studies have implicated partial protein unfolding in the range from +8 to +10 charge state for gaseous cytochrome *c* ions. For example, measurements of the collision cross-sections of the +6 through the +9 ions of bovine cytochrome *c* have been recorded for aqueous electrosprayed solutions (no added acid) by Jarrold and co-workers [60] where a broadening in the drift time distributions from the +8 to +9 charge states of cytochrome *c* was observed, indicating a partial unfolding in the gas-phase due to Coulomb repulsions [61]. Similarly, for electrosprayed solutions of cytochrome *c* containing variable concentrations of

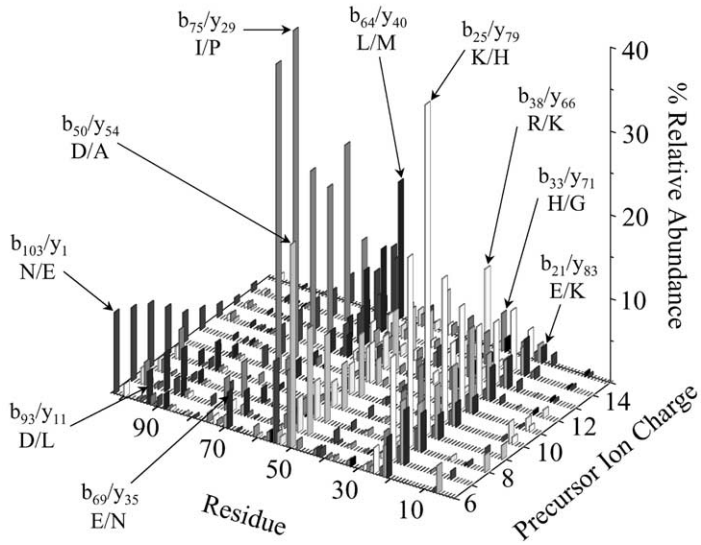

Fig. 4. Dissociation map of ferri-cytochrome *c* as a function of precursor ion charge over a range of $[M + 5H + Fe(III)heme]^{6+}$ to $[M + 14H + Fe(III)heme]^{15+}$ precursor ions. The *x*-axis represents the 104 consecutive amino acid residues within cytochrome *c* where, for example, residue 50 corresponds to an Asp residue, and the b_{50}/y_{54} complementary ion pair. The *z*-axis represents the sum of the ion abundances corresponding to the dissociation of a given amide bond normalized to the sum of the observed product ion abundances.

acetic acid, Jarrold and coworkers noted dramatic changes in the drift time distributions observed for the +9 and +10 ions as acid concentration was increased, while only small changes were noted for the +7 and +8 ions [60]. Several workers have also investigated the methanol and acid induced unfolding of cytochrome *c* at various concentrations of each [62–67]. These results indicate that under the solution conditions used in this study to collect tandem MS data of ferri-cytochrome *c*, the tertiary structure of the protein has been denatured and exists in an "unfolded" state. Nevertheless, the ions must occupy conformational states of varying degrees of compactness, as ion mobility studies show [55], and in addition to total ion charge, the three-dimensional shape of the protein ion is expected to play a major role in defining the Coulomb field of the ion. Whether protein ion conformational changes play a significant role in the observed changes in dissociation behavior remains an open question. However, the N-terminal proline cleavage tends to be particularly important for the relatively high charge states of the protein ions examined thus far [34–36] and might, therefore, be correlated with protein unfolding as a result of Coulomb repulsion. Protonation of the carbonyl oxygen N-terminal to the cleaving Pro residue may effectively initiate local, charge directed fragmentation [32]. The enhanced basicity of this site over other carbonyl sites in the backbone may lead to enhancement of the N-terminal proline cleavage at high charge states in which intramolecular proton transfer to carbonyl groups is otherwise inhibited by the Coulomb field.

The b_{75}/y_{29} N-terminal Pro channel is particularly evident in the product ion spectrum of the +12 ion, shown in the upper panel of Fig. 5, as are several channels at either basic or acidic residues. For this charge state, roughly 37% of the fragmentation is accounted for by basic residue cleavages, 17% by acidic residue cleavages, and 20% by the proline cleavage discussed above. For the precursor ion charge state range from +6 to +14, the dominant cleavage reaction is one of these three types (basic residue, acidic residue, or N-terminal proline cleavage). However, for the highest charge state examined, viz., the ferri-cytochrome

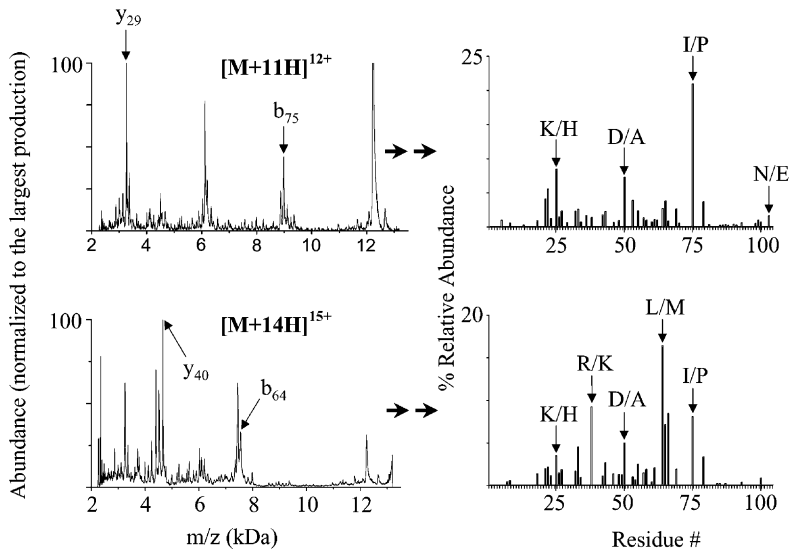

Fig. 5. On the left-hand side is shown the post-ion/ion MS/MS of the $[M + 11H + Fe(III)heme]^{12+}$ and $[M + 14H + Fe(III)heme]^{15+}$ ferri-cytochrome *c* precursor ions where the complementary ion pair of the most dominant amide bond cleavage is labeled. The summed b and y ion plots are as described for Fig. 3.

c +15 ion, the most abundant fragmentation channel gives rise to the b_{64}/y_{40} complementary pair (see Fig. 5). This cleavage corresponds to fragmentation between a leucine residue and a methionine residue. Such a cleavage is not among the commonly observed dominant fragmentation channels for the other charge states. In fact, this precursor ion exhibits the highest percentage of non-specific fragmentation (37%) observed for all charge states studied (basic residues, 33%; Asp and Glu, 20%). It is perhaps significant that the highest apomyoglobin charge states fragment between a leucine residue and a serine residue to yield, by far, the most abundant product complementary pair y_{151}/b_2. The highest charge states studied for cytochrome *c* and apomyoglobin, therefore, show prominent cleavages C-terminal to a leucine residue. Clearly, too few observations are yet available to assess the extent to which these two observations may be related. The various chemical rationale that may be used to explain the enhanced cleavages at acidic, basic, and proline residues may not be readily applied to cleavage C-terminal to leucine residues. However, Breci et al. have reported that proline cleavages are enhanced in peptide ions when valine, isoleucine, or leucine are located N-terminal to the proline residue [68]. This observation is rationalized on the basis of restricted rotational freedom around the peptide linkage, thereby constraining the residues in an orientation conducive to bond cleavage. It remains unclear if a related conformational restriction could play a role in the case of the +15 charge state of cytochrome *c*. However, based on the behavior of apomyoglobin and cytochrome *c*, it is apparent that factors other than those favoring cleavages at basic, acidic, and proline residues can come into play for the "high" precursor ion charge states.

3.6. Comparison of the fragmentation behaviors of apo- and ferri-cytochrome c ions

The role of the heme prosthetic group in the dissociation behavior of cytochrome *c* ions has been discussed by other workers [22]. A general lack of fragmentation near the N-terminal end of the protein, where the heme group is covalently bound through thioether linkages to cysteines 14 and 17, has been

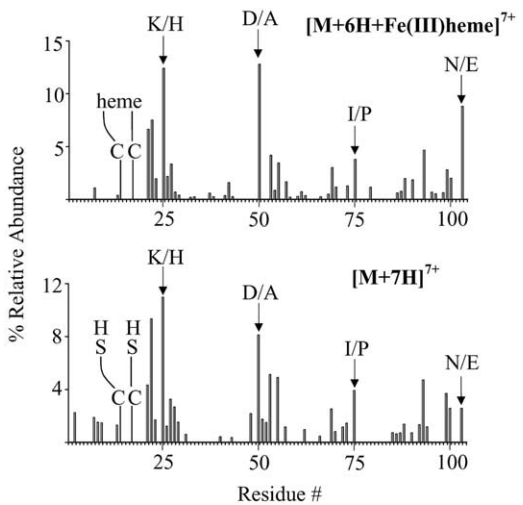

Fig. 6. The upper plot shows the dissociation behavior of the $[M + 6H + Fe(III)heme]^{7+}$ ferri-cytochrome *c* ion where the covalent attachment of the heme group via thioether linkages to Cys 14 and Cys 17 is shown. The lower plot shows the dissociation behavior of the $[M + 7H]^{7+}$ apo-cytochrome *c* ion, showing the absence of heme.

noted. Holo-cytochrome *c* ions show a similar paucity of fragmentation in this region under ion trap collision activation conditions. We, therefore, examined the fragmentation behavior of apo-cytochrome *c* ions to determine what role the presence of the heme group might play in determining the dominant backbone cleavages of the protein under ion trap CID conditions. The summed b and y ion histogram of the +7 charge state of ferri- and apo-cytochrome *c* ions shown in Fig. 6 reveals few differences in the observed dissociation channels of these ions even in the absence of heme. As discussed above, the amide bond cleavages associated with both ferri- and ferro-cytochrome *c* are very similar suggesting that the heme oxidation state has little effect on protein backbone cleavage between the two holo-forms. The apo-cytochrome *c* results also support the proposal that the heme group plays only a subtle role in the observed backbone cleavage results.

Although many similarities exist between the dissociation behaviors of ferri- and apo-cytochrome *c* ions under ion trap collisional activation conditions, some subtle but noticeable differences are evident. Perhaps the most significant difference noted between the fragmentation behaviors of apo- and ferri-cytochrome *c* ions is that for the former ions, more extensive backbone cleavages were observed nearby and adjacent to the dominant dissociation channels than with the latter ions. This is illustrated in Fig. 7, where a comparison of the fragmentation behavior of the +13 ferri-cytochrome *c*, and the +13 apo-cytochrome *c* ions is shown. Evidence is observed for fragmentation at residues 45–52 and 61–71 in the apo-ion, where the former is somewhat centered around the b_{50}/y_{54} C-terminal Asp cleavage, and the latter is centered about the b_{64}/y_{40} Leu–Met cleavage. The holo-ion also exhibits the same dominant cleavages but does not show the extent of cleavage observed within the regions just mentioned for apo-cytochrome *c*. On the other hand, several more or less isolated cleavages are observed for the holo-ion but not for the apo-ion. In the data set presented here, the tandem mass spectrum of any particular ferri- or apo-cytochrome *c* precursor ion charge state shows less than 50% of the 103 amide bonds being cleaved. In a direct comparison for any given precursor ion charge state, it might be difficult to draw firm conclusions regarding the relatively subtle differences apparent in Fig. 7. However, with consideration for all channels observed over the range of charge states common to both apo- and holo-forms studied (+6 to +15), the total sequence coverage is about 70% for the holo-protein, and greater than 80% for the apo-protein. A summary of the dissociation behavior of the apo-cytochrome *c* ions is given in Fig. 8, which can be compared directly with the analogous data for the ferri-cytochrome *c* ions of Fig. 4.

In addition to subtle differences in the observed dissociation channels between apo- and holo-forms of the ions there are differences in the relative abundances of the products. Table 1 summarizes the relative frequencies (in percent total product ion signal where multiple charged ions are not included in the total) of cleavages observed C-terminal to acidic residues, such as Asp and Glu, those C-terminal to basic residues including Arg, Lys, and His, N-terminal Pro cleavages, and all other cleavages, which are designated

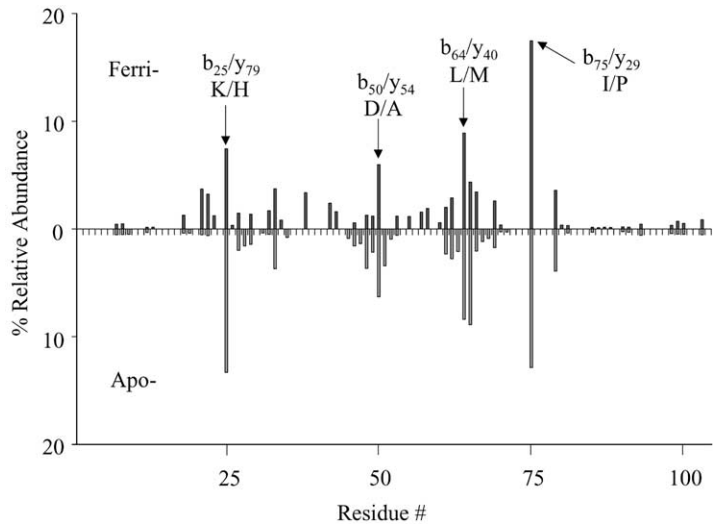

Fig. 7. A mirrored b and y ion plot showing the difference in dissociation behaviors of the +13 charge state of ferri- and apo-cytochrome *c* ions. Many of the peptide bonds surrounding prominent dissociation channels in the holo-oxidized protein remain intact upon CID whereas the apo-protein shows a greater extent of fragmentation in these areas.

as non-specific, as a function of precursor ion charge state. The data presented in Table 1 are derived from an average of 1000 individual scans of each MS/MS spectrum collected for the denoted charge states of ferri- and apo-cytochrome *c* precursor ions. At the low end of the intermediate charge states (i.e., +6 and +7), the Asp and Glu charge-remote dissociation mechanisms show a maximum in their relative contributions.

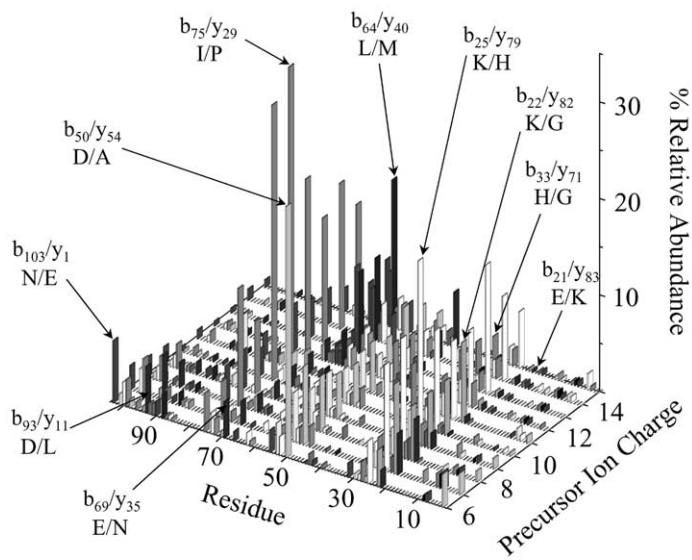

Fig. 8. Dissociation map of apo-cytochrome *c* as a function of precursor ion charge over a range of $[M+6H]^{6+}$ to $[M+15H]^{15+}$ precursor ions. All axes are identical to those in Fig. 4.

Fragmentation at basic residues tends to maximize from +7 to +9 charge states. Proline cleavages show their greatest relative contributions in the range from +10 to +12 and "non-specific" cleavages, which includes the Leu–Met cleavage leading to the b_{64}/y_{40} products discussed above, make the greatest contribution at charge states from +12 to +15 (with the exception of the +6 ferri-cytochrome *c* ion, which shows abundant non-specific cleavage). While the classification used in Table 1 may prove to be too crude to employ as a general tool in accurately predicting the charge state dependent fragmentation behavior of all proteins, it does represent a reasonable starting point, given that the dissociation behaviors of all the proteins studied to date correspond well to the observed trends discussed here.

4. Conclusions

Gaseous cytochrome *c* ions show oxidation state and charge state dependent fragmentation behavior under the quasi-thermal ion activation conditions of the quadrupole ion trap (single frequency resonance excitation). Ferro-cytochrome *c* ions show both protonated heme loss and backbone amide bond cleavages with the former process dominating for the +7 and +8 precursor ions. Ferri-cytochrome *c* ions fragment predominantly via backbone amide bond cleavage for all but the lowest of charge states. Losses of small neutral molecules tend to dominate product ion spectra of the lowest precursor charge states (<+5) for all forms of cytochrome *c* studied.

The identities of the various competitive amide bond cleavages and their dependence upon precursor ion charge state show commonalities with previously reported protein ion dissociation behavior. In general, dominant cleavages tend to be observed C-terminal to acidic residues and C-terminal to basic residues. Cleavages N-terminal to proline residues also give rise to abundant products, depending upon charge state. The relative contributions of the various preferred cleavages are strongly parent ion charge state dependent. A variety of non-specific cleavages at sites other than those mentioned above are also observed, although they are usually of relatively low abundance. A notable exception is the formation of the b_{64}/y_{40} complementary pair resulting from a Leu–Met cleavage, which is the most abundant set of products at relatively high charge states.

Acknowledgements

Research was sponsored by the National Institutes of Health Grant R01-45372 and the U.S. Department of Energy, Office of Basic Energy Sciences Grant DE-FG02-00ER15105.

References

[1] M. Karas, F. Hillenkamp, Anal. Chem. 60 (1988) 2299.
[2] J.F. Mahoney, J. Perel, S.A. Ruatta, P.A. Martino, S. Husain, T.D. Lee, Rapid Commun. Mass Spectrom. 5 (1991) 441.
[3] J.B. Fenn, M. Mann, C.K. Meng, S.F. Wong, C.M. Whitehouse, Science 246 (1989) 64.
[4] S.A. McLuckey, G.J. Van Berkel, G.L. Glish, J. Am. Chem. Soc. 112 (1990) 5668.
[5] P.D. Schnier, D.S. Gross, E.R. Williams, J. Am. Chem. Soc. 117 (1995) 6747.
[6] P.D. Schnier, D.S. Gross, E.R. Williams, J. Am. Soc. Mass Spectrom. 6 (1995) 1086.
[7] M.G. Ikonomou, P. Kebarle, Int. J. Mass Spectrom. Ion Processes 117 (1992) 283.
[8] R.R.O. Loo, B.E. Winger, R.D. Smith, J. Am. Soc. Mass Spectrom. 5 (1994) 1064.
[9] B.E. Winger, K.J. Light-Wahl, R.D. Smith, J. Am. Soc. Mass Spectrom. 3 (1992) 624.
[10] J.L. Stephenson Jr., S.A. McLuckey, Anal. Chem. 69 (1997) 281.
[11] D. Suckau, Y. Shi, S.C. Beu, M.W. Senko, J.P. Quinn, F.M. Wampler, F.W. McLafferty, Proc. Natl. Acad. Sci. U.S.A. 90 (1993) 790.
[12] T.D. Wood, R.A. Chorush, F.M. Wampler, D.P. Little, P.B. O'Connor, F.W. McLafferty, Proc. Natl. Acad. Sci. U.S.A. 92 (1995) 2451.
[13] F.W. McLafferty, Z. Guan, U. Haupts, T.D. Wood, N.L. Kelleher, J. Am. Chem. Soc. 120 (1998) 4732.
[14] S.J. Valentine, D.E. Clemmer, J. Am. Chem. Soc. 119 (1997) 3558.
[15] K.B. Shelimov, M.F. Jarrold, J. Am. Chem. Soc. 118 (1996) 10313.
[16] K.B. Shelimov, D.E. Clemmer, R.R. Hudgins, M.F. Jarrold, J. Am. Chem. Soc. 119 (1997) 2240.
[17] Y. Mao, J. Woenckhaus, J. Kolafa, M.A. Ratner, M.F. Jarrold, J. Am. Chem. Soc. 121 (1999) 2712.

[18] Y. Mao, M.A. Ratner, M.F. Jarrold, J. Phys. Chem B 103 (1999) 10017.
[19] M.F. Jarrold, Acc. Chem. Res. 32 (1999) 360.
[20] Y.-L. Chen, B.A. Collings, D.J. Douglas, J. Am. Soc. Mass Spectrom. 8 (1997) 681.
[21] T.R. Covey, D.J. Douglas, J. Am. Soc. Mass Spectrom. 4 (1993) 616.
[22] D.M. Horn, R.A. Zubarev, F.W. McLafferty, Proc. Natl. Acad. Sci. U.S.A. 97 (2000) 10313.
[23] R.A. Zubarev, D.M. Horn, E.K. Fridriksson, N.L. Kelleher, N.A. Kruger, M.A. Lewis, B.K. Carpenter, F.W. McLafferty, Anal. Chem. 72 (2000) 563.
[24] D.M. Horn, Y. Ge, F.W. McLafferty, Anal. Chem. 72 (2000) 4778.
[25] R.D. Smith, J.A. Loo, C.J. Barinaga, C.G. Edmonds, H.R. Udseth, J. Am. Soc. Mass Spectrom. 1 (1990) 53.
[26] R.D. Smith, C.J. Barinaga, Rapid Commun. Mass Spectrom. 4 (1990) 54.
[27] Y.-T. Li, Y.-L. Hsieh, J.D. Henion, B. Ganem, J. Am. Soc. Mass Spectrom. 4 (1993) 631.
[28] Q. Wu, S. Van Orden, X. Cheng, R. Bakhtiar, R.D. Smith, Anal. Chem. 67 (1995) 2498.
[29] F. He, C.L. Hendrickson, A.G. Marshall, J. Am. Soc. Mass Spectrom. 11 (2000) 120.
[30] N.L. Kelleher, H.Y. Lin, G.A. Valaskovic, D.J. Aaserud, E.K. Fridriksson, F.W. McLafferty, J. Am. Chem. Soc. 121 (1999) 806.
[31] J.R. Yates III, J. Mass Spectrom. 33 (1998) 1.
[32] V.H. Wysocki, G. Tsaprailis, L.L. Smith, L.S. Breci, J. Mass Spectrom. 35 (2000) 1399.
[33] J.M. Wells, J.L. Stephenson Jr., S.A. McLuckey, Int. J. Mass Spectrom. 203 (2000) A1.
[34] T.G. Schaaff, B.J. Cargile, J.L. Stephenson Jr., S.A. McLuckey, Anal. Chem. 72 (2000) 899.
[35] G.E. Reid, J. Wu, P.A. Chrisman, J.M. Wells, S.A. McLuckey, Anal. Chem. 73 (2001) 3274.
[36] K.A. Newton, P.A. Chrisman, G.E. Reid, J.M. Wells, S.A. McLuckey, Int. J. Mass Spectrom. 212 (2001) 359.
[37] J.L. Stephenson Jr., S.A. McLuckey, J. Am. Chem. Soc. 118 (1996) 7390.
[38] J.L. Stephenson Jr., S.A. McLuckey, Anal. Chem. 70 (1998) 3533.
[39] J.M. Wells, G.E. Reid, B.J. Engel, P. Pan, S.A. McLuckey, J. Am. Soc. Mass Spectrom. 12 (2001) 873.
[40] G.J. Van Berkel, G.L. Glish, S.A. McLuckey, Anal. Chem. 62 (1990) 1284.
[41] K.-G. Paul, Acta Chem. Scand. 4 (1950) 239.
[42] J.L. Stephenson Jr., S.A. McLuckey, Int. J. Mass Spectrom. Ion Processes 162 (1997) 89.
[43] S.A. McLuckey, D.E. Goeringer, G.L. Glish, J. Am. Soc. Mass Spectrom. 2 (1991) 11.
[44] J.N. Louris, R.G. Cooks, J.E.P. Syka, P.E. Kelley, G.C. Stafford, J.F.J. Todd, Anal. Chem. 59 (1987) 1677.
[45] J.L. Stephenson Jr., S.A. McLuckey, Anal. Chem. 69 (1997) 3760.
[46] P.E. Kelley, J.E.P. Syka, P.C. Ceja, G.C. Stafford, J.N. Louris, H.F. Grutzmacher, D. Kuck, J.F.J. Todd, in: Proceedings of the Thirty-fourth Conference on Mass Spectrometry and Allied Topics, Cincinnati, OH, 1986, p. 963.
[47] S.A. McLuckey, D.E. Goeringer, J. Mass Spectrom. 32 (1997) 461.
[48] D.E. Goeringer, S.A. McLuckey, J. Chem. Phys. 104 (1996) 2214.
[49] R.A. Jockusch, P.D. Schnier, W.D. Price, E.F. Strittmatter, P.A. Demirev, E.R. Williams, Anal. Chem. 69 (1997) 1119.
[50] D.E. Goeringer, S.A. McLuckey, Int. J. Mass Spectrom. 177 (1998) 163.
[51] K.G. Asano, D.E. Goeringer, D.J. Butcher, S.A. McLuckey, Int. J. Mass Spectrom. 190/191 (1999) 281.
[52] G.J. Van Berkel, F. Zhou, J.T. Aronson, Int. J. Mass Spectrom. Ion Processes 162 (1997) 55.
[53] S.A. McLuckey, J.L. Stephenson Jr., Mass Spectrom. Rev. 17 (1998) 369.
[54] W.D. Price, P.D. Schnier, E.R. Williams, Anal. Chem. 68 (1996) 859.
[55] G. Tsaprailis, H. Nair, A. Somogyi, V.H. Wysocki, W.Q. Zhong, J.H. Futrell, S.G. Summerfield, S.J. Gaskell, J. Am. Chem. Soc. 121 (1999) 5142.
[56] C.G. Gu, A. Somogyi, V.H. Wysocki, K.F. Medzihradszky, Anal. Chim. Acta 39 (1999) 247.
[57] C.G. Gu, G. Tsaprailis, L. Breci, V.H. Wysocki, Anal. Chem. 72 (2000) 5804.
[58] G. Tsaprailis, A. Somogyi, E.N. Nikolaev, V.H. Wysocki, Int. J. Mass Spectrom. 196 (2000) 467.
[59] http://webbook.nist.gov, NIST Chemistry WebBook, NIST Standard Reference Database #69, February (2000) Release.
[60] R.R. Hudgins, J. Woenckhaus, M.F. Jarrold, Int. J. Mass Spectrom. Ion Processes 165/166 (1997) 497.
[61] D.E. Clemmer, R.R. Hudgins, M.F. Jarrold, J. Am. Chem. Soc. 117 (1995) 10141.
[62] K.R. Babu, A. Moradian, D.J. Douglas, J. Am. Soc. Mass Spectrom. 12 (3) (2001) 317.
[63] L. Konermann, D.J. Douglas, Biochemistry 36 (40) (1997) 12296.
[64] S.K. Chowdhury, V. Katta, B.T. Chait, J. Am. Chem. Soc. 112 (1990) 9012.
[65] F. Boffi, A. Bonincontro, S. Cinelli, et al., Biophys. J. 80 (3) (2001) 1473.
[66] Y.O. Kamatari, T. Konno, M. Kataoka, K. Akasaka, J. Mol. Biol. 259 (3) (1996) 512.
[67] S. Ideue, K. Sakamoto, K. Honma, D.E. Clemmer, Chem. Phys. Lett. 337 (1–3) (2001) 79.
[68] L. Breci, V.H. Wysocki, in: Proceedings of the Forty-ninth ASMS Conference on Mass Spectrometry and Allied Topics, Chicago, IL, May 27–31, 2001.